Multiresolution stochastic simulations of reaction–diffusion processes

Basil Bayati, Philippe Chatelain and Petros Koumoutsakos*

Received 25th June 2008, Accepted 5th August 2008
First published as an Advance Article on the web 1st September 2008
DOI: 10.1039/b810795e

Stochastic simulations of reaction–diffusion processes are used extensively for the modeling of complex systems in areas ranging from biology and social sciences to ecosystems and materials processing. These processes often exhibit disparate scales that render their simulation prohibitive even for massive computational resources. The problem is resolved by introducing a novel stochastic multiresolution method that enables the efficient simulation of reaction–diffusion processes as modeled by many-particle systems. The proposed method quantifies and efficiently handles the associated stiffness in simulating the system dynamics and its computational efficiency and accuracy are demonstrated in simulations of a model problem described by the Fisher–Kolmogorov equation. The method is general and can be applied to other many-particle models of physical processes.

Introduction

Spatially distributed stochastic simulations of reaction–diffusion processes are frequently used for the modeling of physical phenomena ranging from biology and social sciences to ecosystems and materials processing. Indeed spatial dynamics, such as wavefront propagation and pattern formation, are intrinsic to physical phenomena ranging from morphogenesis[1] and pedestrian traffic[2] to epitaxial growth[3] and epidemics.[4] Reaction–diffusion models of these phenomena often involve microscopic simulations using many-particle systems. The evolution of these systems can be modeled stochastically using algorithms known as the BKL[5] or the stochastic simulation algorithm (SSA).[6] These methods were originally developed for homogeneous systems and their extension to spatially inhomogeneous systems is associated with a high computational cost. Spatially inhomogeneous, stochastic simulation methods divide the volume into uniform cells with reactions occurring within cells and diffusion events modeled as unimolecular transitions to neighboring cells. A number of recent works have employed such algorithms to simulate reaction–diffusion processes of biological systems[7–10] using a uniform discretization of the computational domain. In these simulations, the finest spatial scales dictate the size of the cells, thus making the method highly inefficient in areas where coarser scales are operating. We note that simulations of these systems are impossible even when employing massively parallel computer architectures. In order to overcome this difficulty, novel multiscale methods have been proposed,[11–13] which combine stochastic, microscopic, deterministic, and coarse-grained descriptions.

Chair of Computational Science, CH-8092 ETH Zurich, Switzerland. E-mail: petros@ethz.ch

In this Communication, we present a novel multiresolution method for the efficient stochastic simulation of reaction–diffusion processes for spatially developing systems. The method entails discretizing the computational domain into cells of different sizes in the spirit of adaptive mesh refinement (AMR),[14,15] which was developed for the discretization of partial differential equations. The proposed multiresolution algorithm enables the stochastic handling of phenomena with disparate spatial scales, but at the same time it leads to a temporal disparity that increases the complexity of the simulations. We solve this problem by combining approximate, accelerated stochastic simulation algorithms[16,17] with the AMR technique. We note that, to the best of our knowledge, no algorithm for multiresolution stochastic simulations has been developed. In this work we quantify the scale disparity and the proposed algorithm is validated in simulations of one-dimensional wavefront propagation in a model reaction–diffusion system described by the Fisher–Kolmogorov equation.[18] The results demonstrate the need and the effectiveness of multiresolution simulations for inhomogeneous reaction–diffusion processes.

The method

The governing reaction–diffusion processes are simulated using a stochastic particle description where particles in a computational domain, discretized by a series of meshes, move *via* Brownian motion and are subject to molecular collisions. In the present spatial simulations, the domain is decomposed into independent cells such that a reactant molecule can only react with other reactants in its cell, while diffusion events are modeled as unimolecular transitions to neighboring cells.

We consider a set of one-dimensional meshes indexed by an integer $\mathscr{L}$, with $\mathscr{L} = 0$ denoting the coarsest mesh, and the finer meshes denoted by increasing positive integers, such that the cell spacing for mesh level $\mathscr{L} + 1$ is half of that for level $\mathscr{L}$. Reaction-diffusion processes can be expressed in a unified framework in terms of generic transitions:

$$\sum_{j=1}^{N} \alpha_{z,j} A_{i,j}^{\mathscr{L}_j} \rightarrow \sum_{j=1}^{N} \beta_{z,j} A_{k,j}^{\mathscr{L}_k}, \qquad (1)$$

where N is the total number of species, $\alpha_{z,j}$ and $\beta_{z,j}$ are the stoichiometric values for transition index z for species j, and $A_{i,j}^{\mathscr{L}_i}$ represents the species j at cell index i at mesh level $\mathscr{L}_i$.

In the context of a multiresolution representation, the computational elements are mapped onto different levels of discretization corresponding to different mesh resolutions. This enables the efficient use of computational elements, since we can place larger numbers of computational elements in areas of the domain associated with fine spatial scales (*e.g.* around a propagating front), while other areas are discretized

using fewer computational elements. This representation requires communication between different discretization levels, a process that is facilitated by the discrete nature of the particles.

We let $U_i^{\mathscr{L}_i}$ denote the number of particles at cell index i on mesh level $\mathscr{L}_i$. The refinement of the computational elements for a species $U_i^{\mathscr{L}_i}$ from level $\mathscr{L}_i$ to level $\mathscr{L}_i + 1$ is performed as:

$$U_{2i}^{\mathscr{L}_i+1} \sim B\left(U_i^{\mathscr{L}_i}, \frac{1}{2}\right), \tag{2}$$

$$U_{2i+1}^{\mathscr{L}_i+1} \sim B\left(U_i^{\mathscr{L}_i} - U_{2i}^{\mathscr{L}_i+1}, \frac{1/2}{1-1/2}\right) = U_i^{\mathscr{L}_i} - U_{2i}^{\mathscr{L}_i+1}, \tag{3}$$

where $\mathscr{B}(N,p)$ represents a binomial distribution of N independent trials with a success rate of p, and we note that eqn (3) represents a conditional distribution.

The coarsening of computational elements from level $\mathscr{L}_i + 1$ to $\mathscr{L}_i$ is performed by

$$U_i^{\mathscr{L}_i} = U_{2i}^{\mathscr{L}_i+1} + U_{2i+1}^{\mathscr{L}_i+1}. \tag{4}$$

Temporal scale disparity, diffusion propensities

We define $a_{D,i,j}^{\mathscr{L}_i,\mathscr{L}_i}$ as the diffusion propensity from cell i on level $\mathscr{L}_i$ to cell j on level $\mathscr{L}_j$, where j is a neighboring cell to i:

$$a_{D,i,j}^{\mathscr{L}_i,\mathscr{L}_j} = U_i^{\mathscr{L}_i}\kappa(\mathscr{L}_i, \mathscr{L}_j). \tag{5}$$

The diffusion rate, $\kappa(\mathscr{L}_i,\mathscr{L}_j)$, can be derived by virtue of a finite volume approximation as shown in ref. 9, and is given as:

$$\kappa(\mathscr{L}_i, \mathscr{L}_j) = \frac{2\nu}{h(\mathscr{L}_i)(h(\mathscr{L}_i) + h(\mathscr{L}_j))}, \tag{6}$$

where $h(\mathscr{L})$ is the cell spacing at level $\mathscr{L}$ and ν is the diffusion coefficient. Using the partial sum for a geometric series and eqn (5)–(6), the mean change in propensities with respect to the coarsest level is:

$$a_{\mathrm{D},i'j'}^{\mathscr{L}_{i'},\mathscr{L}_{j'}} = a_{\mathrm{D},i,j}^{0,0}\zeta(\mathscr{L}_{i'}, \mathscr{L}_{j'}), \tag{7}$$

where

$$\zeta(\mathscr{L}_i, \mathscr{L}_j) = \begin{cases} 2^{\mathscr{L}_i} & \text{if } \mathscr{L}_i = \mathscr{L}_j \\ \frac{2^{\min(\mathscr{L}_i,\mathscr{L}_j)}}{\frac{1}{2}+2^{-|\mathscr{L}_i-\mathscr{L}_j|-1}} & \text{otherwise.} \end{cases} \tag{8}$$

Eqn (7)–(8) show that non-uniform cell sizes introduce disparities in the diffusion propensities since finer cells exhibit faster diffusion rates compared with coarser cells.

Temporal scale disparity, reaction and diffusion propensities

Stiffness, which is a disparity in time-scales, is present in most stochastic, homogeneous chemical systems.[19,20] Here we show that, by decreasing the cell size in a uniform discretization for inhomogeneous systems, the reaction and diffusion propensities become progressively disparate. Consequently, this forces exact stochastic simulation algorithms[6,21] to spend more time sampling diffusion events than reaction events. This resolution-dependent stiffness warrants the efficient allocation of computational resources, such as adaptive meshes since the finest spatial scales are often localized in the domain.

We denote the dimension of the problem by d, and define a characteristic length scale h_λ for each level of discretization such that:

$$h_\lambda = \frac{L_0}{2^\lambda}, \tag{9}$$

where $\lambda \geq 0$ and L_0 is the length of the domain. Additionally, we define the number of particles of species s when $\lambda = 0$ to be X_s and the corresponding concentration of species s to be $\chi_s = X_s/V_\lambda \leq 1$, where V_λ is a normalization factor that depends on λ. Employing eqn (5)–(6) and noting that the number of particles in a cell is proportional to the cell size, the maximum diffusion propensity for a species X_1 is given as:

$$\hat{a}_\mathrm{D} = (X_1 h_\lambda^d)\left(\frac{\nu}{h_\lambda^2}\right) = X_1 \nu L_0^{d-2} 2^{2\lambda-\lambda d}. \tag{10}$$

In this Communication, without loss of generality, we consider a representative set of bimolecular reactions (frequently encountered in chemical kinetics and phase transition problems) such as the Fisher–Kolmogorov equation in ref. 18, originally proposed as a model for the propagation of a gene in a population. This equation models reaction–diffusion processes admitting traveling wave solutions. The continuum form of this equation for the two species involved, χ_1 and χ_2, reads:

$$\frac{\partial \chi_1}{\partial t} - \nu\Delta\chi_1 = k\chi_1\chi_2 = k(\chi_1 - \chi_1^2), \tag{11}$$

where k is the deterministic reaction rate and the conservation relation, $\chi_1 + \chi_2 = 1$, has been used. If the initial condition of eqn (11) satisfies $0 \leq \chi_1(x,0) \leq 1$, $\chi_1(x,0) = 1$ for $x < a$, $\chi_1(x,0) = 0$ for $x > b$, where $a < b$, then the solution is a traveling wave with a constant wavespeed.[22] In cases of low particle concentrations, the continuum equation can be replaced by its equivalent discrete form:

$$X_1 + X_2 \rightarrow 2X_1, \tag{12}$$

where X_1 and X_2 are both diffusing species. The propensity for any such biomolecular reaction can be written as

$$\hat{a}_\mathrm{R} = (X_1 h_\lambda^d)(X_2 h_\lambda^d)\left(\frac{k}{V_\lambda}\right). \tag{13}$$

The concentration of X_2 is obtained from eqn (13),

$$\chi_2 = \frac{X_2 h_\lambda^d}{V_\lambda} \leq 1, \tag{14}$$

thus, the maximum reaction propensity is (*cf.* eqn (10))

$$\hat{a}_\mathrm{R} = {X_1}^k {L_0}^d 2^{-\lambda d}. \tag{15}$$

To estimate the relative disparity between reaction and diffusion propensities, we define a dimensionless scaling parameter $\hat{\xi}(\lambda)$ where

$$\hat{\xi}(\lambda) = \frac{\hat{a}_\mathrm{D}}{\hat{a}_\mathrm{R}} = \frac{2^{2\lambda}}{L_0^2}\left(\frac{\nu}{k}\right), \lambda \geq 0. \tag{16}$$

We observe that $\hat{\xi}(\lambda)$ is independent of the dimensionality of the problem, d. The finite volume approximation of the propensities in eqn (5)–(6) scales with $\mathscr{O}({h_\lambda}^2)$[9] thus, accurate

simulations of the diffusion process engenders temporal scale disparities. The numerical value quantifying this scale-disparity is

$$\xi(\lambda) = \frac{\max_i(a_{D,i,j}^{\mathscr{L}_i,\mathscr{L}_j})}{\max_i(a_{R,i}^{\mathscr{L}_i})}, \qquad (17)$$

where $a_{D,i,j}^{\mathscr{L}_i,\mathscr{L}_j}$ is the diffusion propensity defined in eqn (5)–(6), and $a_{R,i}^{\mathscr{L}_i}$ is the reaction propensity for cell i on level $\mathscr{L}_i$.[6,21] In Fig. 1, we show $\hat{\xi}(\lambda)$ and $\xi(\lambda)$ plotted against h_λ, which represents the temporal scale disparity of the Fisher–Kolmogorov equation for $\nu = 1/160^2$, $k = 1$ and $L_0 = 1$. It can be seen that as h_λ decreases, the ratio of the diffusion to reaction propensities increases, thus leading to a stiffer system.

Numerical results

The Fisher–Kolmogorov equation exhibits a localization of fine spatial scales in the form of a traveling wave. To demonstrate the validity of the present method, we simulated the Fisher–Kolmogorov equation (see eqn (11)–(12)) with $\nu = 1/160^2$, $k = 1$, on the domain $x \in [-1/4, 3/4]$, using approximate, accelerated stochastic simulation algorithms.[16,17] The analytical solution for the continuum form of the Fisher–Kolmogorov (eqn (11)) is:[22,23]

$$\chi_1(x,t) = \frac{1}{(1 + ae^{b(x-ct)})^2}, \qquad (18)$$

where $a = \sqrt{2} - 1$, $b = 80\sqrt{2/3}$, and the wavespeed $c = 1/(32\sqrt{6})$. Eqn (18) was used to generate an initial condition with a total of 8×10^6 particles in the domain. Consequently, the shape of the wave, save for fluctuations, remains the same so that the error with respect to the velocity could be determined. We used four types of discretizations for comparison: three uniform meshes and one multiresolution mesh. The cell sizes were $h_\lambda = 2.5 \times 10^{-2}$, 1.25×10^{-2}, and 6.25×10^{-3} for the uniform meshes, and $\min(h_\lambda) = 6.25 \times 10^{-3}$ and $\max(h_\lambda) = 2.5 \times 10^{-2}$ for the multiresolution mesh. We note that these values are also used to show the scale-disparity in Fig. 1. Simulations were performed until $t = t_{\text{end}} = 19.6$. The multiresolution mesh was refined and coarsened according to

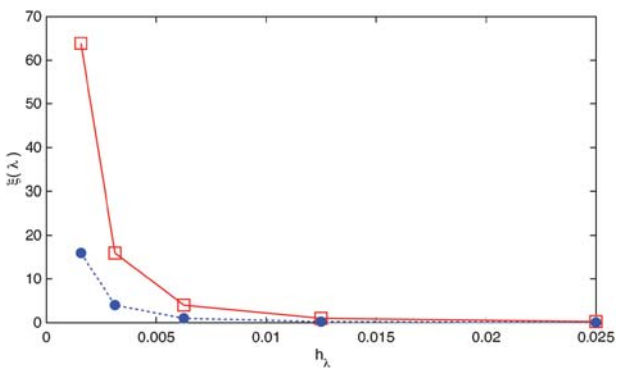

Fig. 1 Scale-disparity of Fisher–Kolmogorov equation: ratio of the maximum diffusion propensity to the maximum reaction propensity plotted against the cell size, h_λ. '– – ● – –' denotes the estimated value, $\hat{\xi}(\lambda)$ (eqn (16)), '—□—' denotes the numerical value, $\xi(\lambda)$ (eqn (17)) for $\nu = 1/160^2$, $k = 1$ and $L_0 = 1$.

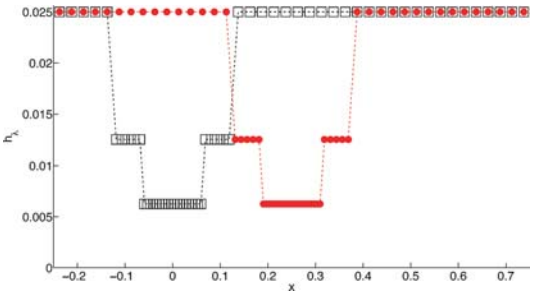

Fig. 2 Multiresolution mesh for the Fisher–Kolmogorov simulation: cell size h_λ against position, where '– –□– –' is the resolution at $t = 0$ and '– –●– –' at $t = t_{\text{end}} = 19.6$. Wavefront center at t_{end} is $x = 1/4$.

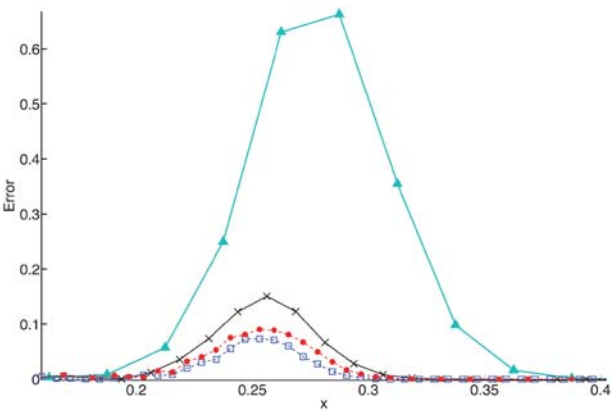

Fig. 3 Error of Fisher–Kolmogorov simulation: pointwise error with respect to the analytical solution against the position. '—▲—', '—X—', '– –□– –' uniform methods with $h_\lambda = 2.5 \times 10^{-2}$, 1.25×10^{-2}, 6.25×10^{-3}, respectively. '– –●– –' multiresolution method with $\min(h_\lambda) = 6.25 \times 10^{-3}$ and $\max(h_\lambda) = 2.5 \times 10^{-2}$. Wavefront center at $t = t_{\text{end}} = 19.6$ is $x = \frac{1}{4}$ for the analytical solution.

eqn (2)–(4) using *a priori* knowledge of the wavespeed. In Fig. 2, the initial and final multiresolution meshes are shown, where the initial mesh was centered around $x = 0$ and the final mesh around $x = 1/4$. The Figure also indicates that a total of three levels were used for the simulation.

Fig. 3 shows the pointwise error of the four simulations with respect to the analytical solution of the Fisher–Kolmogorov equation (eqn (18)) at $t = t_{\text{end}} = 19.6$. The error indicates the effect of the discretizations with respect to the wavespeed. The coarsest uniform discretization clearly has an inaccurate wavespeed, while the multiresolution method displays an accuracy comparable to the uniform method with $h_\lambda = 6.25 \times 10^{-13}$, and yet it requires approximately 67% less computational time. The Gaussian-like shape of the error reveals that the center of the wave is a critical part of the chemical system. The center of the wavefront for the analytical solution is $x = 1/4$.

Concluding remarks

We presented a novel framework for multiresolution stochastic simulations of reaction–diffusion processes exhibiting disparate scales. The framework relies on the efficient combination of multiresolution discretizations to capture the disparate spatial scales of reaction–diffusion processes, and novel accelerated

stochastic simulation algorithms capable of resolving the resulting scale disparities. The results indicate that the present framework can address the simulation of reaction–diffusion processes that would be impossible to simulate even with massive computational resources. The proposed methodology is general and applicable in a wide range of spatial stochastic many-particle models of physical processes ranging from social systems to biology. Future work includes extending the framework for 2- and 3-dimensional problems and developing robust refinement and coarsening criteria.

References

1 A. Turing, *Philos. Trans. R. Soc. London, Ser. B*, 1952, **1**, 1.
2 D. Helbing, *Rev. Mod. Phys.*, 2001, **73**(4), 1067–1141.
3 M. Copel, M. C. Reuter, E. Kaxiras and R. M. Tromp, *Phys. Rev. Lett.*, 1989, **63**(6), 632–635.
4 K. Dietz, *J. R. Stat. Soc., Ser. A*, 1967, **130**, 505–528.
5 A. B. Bortz, M. H. Kalos and J. L. Lebowitz, *J. Comput. Phys.*, 1975, **17**(1), 10–18.
6 D. T. Gillespie, *J. Comput. Phys.*, 1976, **22**(4), 403–434.
7 J. Hattne, D. Fange and J. Elf, *Bioinformatics*, 2005, **21**(12), 2923–2924.
8 J. Rodriguez, J. Kaandorp, M. Dobrzynski and J. Blom, *Bioinformatics*, 2006, **22**(15), 1895–1901.
9 D. Bernstein, *Phys. Rev. E: Stat., Nonlinear, Soft Matter Phys.*, 2005, **71**(4), 041103.
10 D. Rossinelli, B. Bayati and P. Koumoutsakos, *Chem. Phys. Lett.*, 2008, **451**(1–3), 136–140.
11 I. G. Kevrekidis, C. W. Gear and G. Hummer, *AIChE J.*, 2004, **50**(7), 1346–1355.
12 P. Koumoutsakos, *Annu. Rev. Fluid Mech.*, 2005, **37**, 457–487.
13 A. Hellander and P. Lotstedt, *J. Comput. Phys.*, 2007, **227**(1), 100–122.
14 M. J. Berger and J. Oliger, *J. Comput. Phys.*, 1984, **53**(3), 484–512.
15 M. J. Berger and P. Colella, *J. Comput. Phys.*, 1989, **82**(1), 64–84.
16 D. Gillespie, *J. Chem. Phys.*, 2001, **115**(4), 1716–1733.
17 A. Auger, P. Chatelain and P. Koumoutsakos, *J. Chem. Phys.*, 2006, **125**(8), 084103.
18 R. Fisher, *Ann. Eugenics*, 1937, **7**, 355–369.
19 Y. Cao, D. T. Gillespie and L. R. Petzold, *J. Chem. Phys.*, 2007, **126**(22), 224101.
20 M. Rathinam, L. R. Petzold, Y. Cao and D. T. Gillespie, *J. Chem. Phys.*, 2003, **119**(24), 12784–12794.
21 D. Gillespie, *J. Phys. Chem.*, 1977, **81**(25), 2340–2361.
22 M. J. Ablowitz and A. Zeppetella, *Bull. Math. Biol.*, 1979, **41**(6), 835–840.
23 J. Murray, *Mathematical Biology: An Introduction*, Springer-Verlag, 2002.